

A note on the Li–Cu–O system

R. Berger*

Department of Inorganic Chemistry, Materials Science Centre, University of Groningen, Nijenborgh 16, 9747 AG Groningen (The Netherlands)

(Received August 22, 1990)

Abstract

In the Li–Cu–O system two new ternary phases have been found, tentatively described by the stoichiometries LiCu_3O_3 and LiCu_2O_2 , and both containing Cu^{I} and Cu^{II} . They exhibit p-type “hopping” conduction owing to localized charge carriers. Their powder patterns are successfully indexed on high-symmetry cells where the dimensions depend on a slightly variable stoichiometry. LiCu_3O_3 is tetragonal with $a = 2.815 (\sqrt{2}) \text{ \AA}$ and $c = 8.88 \text{ \AA}$. LiCu_2O_2 is orthorhombic with $a = 5.72 \text{ \AA}$, $b = 2.86 \text{ \AA}$ and $c = 12.4 \text{ \AA}$.

$\text{Li}_3\text{Cu}_2\text{O}_4$, containing Cu^{II} and Cu^{III} , is indexed on a C-centred monoclinic cell: $a = 9.958 \text{ \AA}$, $b = 2.777 \text{ \AA}$, $c = 7.281 \text{ \AA}$ and $\beta = 118.77^\circ$.

The solubility of lithium in CuO is maximally $\text{Li}_{0.06}\text{Cu}_{0.94}\text{O}$ for supersaturation at 1100 K. The equilibrium solubility limit is about $\text{Li}_{0.02}\text{Cu}_{0.98}\text{O}$, for which the solid solution is still semiconducting. The temperature dependence of the magnetic susceptibility is similar to that of pure CuO but T_N is considerably lower.

1. Introduction

While the 3d transition metal monoxides having the NaCl structure tolerate doping by lithium to a large extent, CuO does not. Hauffe and Grunewald [1], and Heikes and Johnston [2] give a maximum of 2 mol% solubility. Silakov *et al.* [3] discuss figures of up to 20% which seem dubious.

On the other hand, the Li–Cu–O system is interesting from a crystal chemical point of view considering that the coordination numbers (CN) with oxygen as ligand vary for lithium (CN 4, 5 or 6) as well as for copper (CN 2, 4, 5, or 6), the latter metal obviously through the possibility of valence change. The ternary phases occurring may be classified with the valence value of copper as a basis.

Cu^{II} (CN 4) is found in Li_2CuO_2 [4, 5] and Cu^{I} (CN 2) in $\text{Li}_4\text{Cu}_4\text{O}_4$ [6] where lithium has a tetrahedral oxygen coordination. In addition, ternary phases have been found where copper occurs with a higher valence than two—at least formally. The structure of Li_3CuO_3 [7] is known while less characterized products have been ascribed the stoichiometries Li_5CuO_4 [8], $\text{Li}_3\text{Cu}_2\text{O}_4$ [9] and $\text{Li}_{1.5}\text{CuO}_2$ [10]. The two latter phases have been synthesized in different manners. Judging from their

*On leave from Uppsala University, Sweden.

powder diffraction data, they are not identical. A compound “ LiCuO_2 ”, stoichiometrically analogous to NaCuO_2 and KCuO_2 [11], has not, as yet, been found.

The present work reports on two new ternary phases containing $\text{Cu}^{\text{I}}/\text{Cu}^{\text{II}}$ and contains supplementary data to previous findings.

2. Experimental details

The solid solutions and most of the compounds were prepared at high temperatures by reacting CuO with Li_2CO_3 in air or oxygen at ambient pressure using alumina as the crucible material. Only at temperatures above 1300 K was chemical attack on the crucible wall observed, through $\gamma\text{-LiAlO}_2$ formation. $\text{Li}_3\text{Cu}_2\text{O}_4$ was synthesized at 570 K from a mixture of Li_2O and CuO together with Ag_2O in a silver ampoule. On decomposition of Ag_2O , present in the form of a powder compact not in contact with the reacting oxide mixture, an elevated oxygen pressure is obtained. The silver container was made by mechanically tightening the ends of a silver tube (Heraeus Edelmetalle GmbH) by pinching and folding.

All samples were investigated by film technique using a $\text{Cu K}\alpha_1$ Guinier-Hägg camera. The line positions were calibrated against silicon ($a = 5.431028 \text{ \AA}$ at 296 K [12]). The new patterns were indexed on the basis of tentative models arrived at by an analysis of the ΔQ matrix (recurring values when taking all possible differences) or by using an automatic indexing program. The thermal decomposition of the new phases was studied with a Guinier-Simon powder camera.

The lithium-rich carbonate/oxide mixtures were investigated using a SEIKO SSC5000 TG/DTA (thermogravimetry/differential thermal analysis) system. This procedure served as a basis for choosing correct reaction temperatures and gave, together with sampling at a constant temperature for X-ray diffraction analysis, information on the reactions occurring on heating the mixtures or single phases. The cooling cycle was also studied in some cases. The temperature change was linear, $10\text{--}20 \text{ K min}^{-1}$.

The equipment for studying the temperature dependence of electrical resistivity and thermoelectric effect has been described previously [13]. Where crystals of large size were not available powder compacts were used with platinum paint for contacts. For the magnetic susceptibility measurements the Faraday technique was used (details of the equipment may be found in ref. 13).

3. Results

3.1. The solid solution $\text{Li}_x\text{Cu}_{1-x}\text{O}$

Substitution of lithium in CuO is likely to cause only small changes in the cell parameters considering the relative magnitudes of the ionic radii of Li^+ and Cu^{2+} . Analysis of the cell parameters reveals that, on increasing the lithium content, the b and c axes decrease while the a axis and the β angle increase. The total effect on the volume is a slight decrease. The ionic radius of lithium is slightly larger than

TABLE 1

Comparison between cell parameters obtained for CuO and $\text{Li}_x\text{Cu}_{1-x}\text{O}$, the latter representing maximum solubility of lithium in a mixture together with Li_2CuO_2 . The figures within parentheses denote the estimated standard deviations

	a (Å)	b (Å)	c (Å)	β (deg)	V (Å ³)	Reference
CuO	4.6837(5)	3.4226(5)	5.1288(6)	99.54(1)	81.08	16
	4.684(2)	3.422(2)	5.123(2)	99.60(1)	80.96	17
	4.6887(9)	3.4248(8)	5.1321(8)	99.55(2)	81.27	18
	4.6881(6)	3.4245(8)	5.1312(9)	99.51(1)	81.25	This work
	4.6911(4)	3.4220(4)	5.1363(5)	99.34(1)	81.36	This work
$\text{Li}_x\text{Cu}_{1-x}\text{O}$	4.6969(4)	3.4073(5)	5.1239(5)	99.72(1)	80.82	This work

that of Cu^{2+} , but since the cations are not isovalent holes are created and these cause an effective attraction in the lattice. Lattice parameter values, also from the literature [16–18], are given in Table 1.

That positive charge carriers are indeed present can be seen from the thermoelectric data. The Seebeck coefficient (α) is positive and decreases on lithium substitution. The temperature (T) dependence of α is neither linear in T (metallic) nor in T^{-1} (semiconducting) for the solid solutions. Resistivity data suggest that $\text{Li}_x\text{Cu}_{1-x}\text{O}$ are semiconducting ($\log \rho$ vs. T^{-1} is linear), and the activation energy decreases with increasing x . A solubility limit $x=0.02$ was estimated from X-ray diffraction phase analysis on samples quenched from 1100 K.

The parent compound, CuO, shows antiferromagnetic ordering at 230 K as judged from neutron diffraction [14] and indicated by the point of steepest descent in the temperature dependence of the magnetic susceptibility [15]. Similar conclusions may be drawn for the lithium-substituted material, except that T_N is lowered considerably (Fig. 1).

3.2. The tie-line Li_2CuO_2 – $\text{Li}_x\text{Cu}_{1-x}\text{O}$

Figure 2 illustrates a typical thermogram of a $\text{Li}_2\text{CO}_3/\text{CuO}$ mixture. On heating, the mass is constant up to approximately 900 K, where mass is lost until a new plateau appears approximately 200 K higher. The natural interpretation is to assign the change to CO_2 evolved from dissociation of the carbonate. Pure Li_2CO_3 decomposes at much higher temperatures after melting at 732 °C [19]. Therefore, the mass loss is effected by an accompanying reaction between the components.

The TG signal and its temperature derivative change smoothly with temperature in this range, while the DTA signal shows an endothermic peak superimposed on the heat effect due to the combination reaction. The extra peak corresponds to the melting of unreacted Li_2CO_3 . Presumably, a change in heating rate would affect the size of this peak.

The mass loss within a series of different $\text{Li}_2\text{CO}_3/\text{CuO}$ ratios is significantly less than that expected from CO_2 loss alone. Assuming that the carbonate dissociation is complete, the reaction must involve a small compensation in mass, *i.e.* oxygen

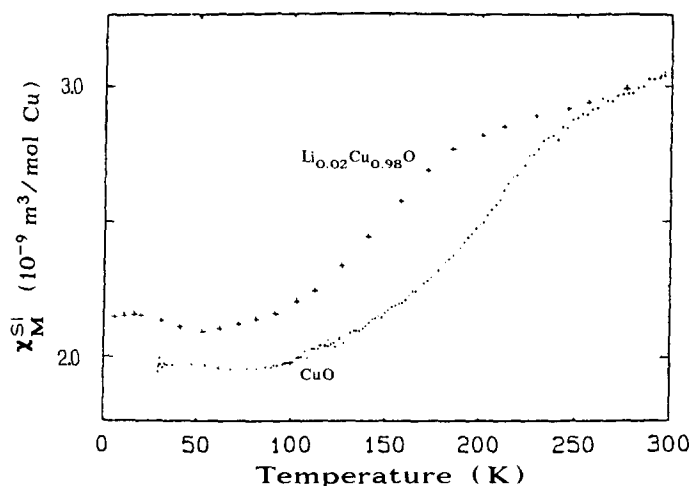


Fig. 1. A comparison between the magnetic susceptibilities of pure CuO and a solid solution with lithium. The data for CuO were taken from ref. 15.

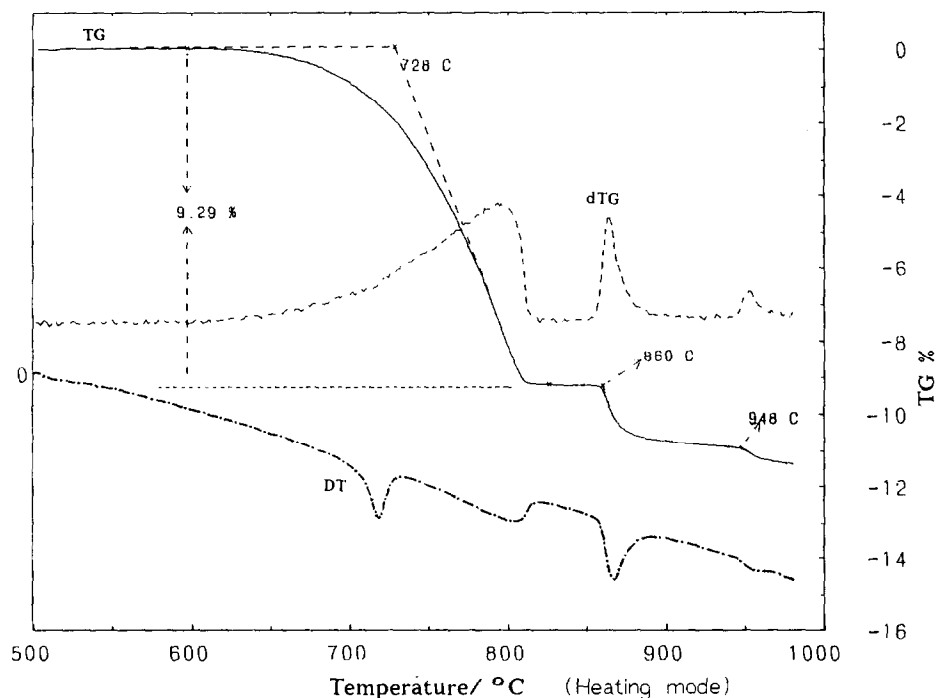


Fig. 2. TG/DTA thermogram of a $\text{Li}_2\text{CO}_3/\text{CuO}$ mixture corresponding to $\text{Li}:\text{Cu}=3:7$. A 10 mg sample was heated from room temperature at a rate of 20 K min^{-1} in a 50 ml min^{-1} oxygen flow. Full line, TG signal; broken line, its time derivative; chain line, DT signal. The data (DTA, TG, temp.) were sampled simultaneously at a rate of 10 s^{-1} .

TABLE 2

Nominal end concentrations obtained from TGA after Li_2CO_3 decomposition (~ 1100 K) for different starting mixtures $\text{Li}_2\text{CO}_3/\text{CuO}$, $y = x_{\text{Li}}/(x_{\text{Li}} + x_{\text{Cu}})$, assuming that the observed mass loss is a combination of CO_2 exhaust and O_2 uptake

y	CO_2 loss % (Theor.)	Total loss % (Exp.)	Ratio Exp./theor.	Concentrations at plateau		
				x_{Li}	x_{Cu}	x_{O}
0.200	6.19	5.65	0.913	0.104	0.416	0.480
0.249	7.95	7.57	0.952	0.132	0.397	0.471
0.298	9.81	9.29	0.947	0.159	0.375	0.466
0.349	11.87	11.41	0.961	0.189	0.354	0.457
0.399	14.03	13.45	0.959	0.219	0.330	0.451

is taken up. Data from a series of measurements are given in Table 2, where the final compositions at the plateaux were calculated assuming that the observed mass difference corresponds with oxygen concentration.

In a separate series of experiments, the same mixtures as in the TG/DTA series were kept at 1100 K (at the plateau in the thermogram) and were sampled for X-ray powder diffraction at various intervals. The situation after 5–10 min, mimicking the timescale of the TG/DTA experiment, corresponds to a binary mixture of $\text{Li}_x\text{Cu}_{1-x}\text{O}$ and Li_2CuO_2 .

The points of composition in the ternary phase diagram seem to be situated on a straight line which also includes the latter phase. The line is thus a tie-line in the phase diagram fixed at the point $(x_{\text{O}}, x_{\text{Li}}) = (\frac{2}{5}, \frac{2}{5})$. Its analytical form may be determined in a one-parameter problem by a least-squares treatment, writing the equation of the tie-line as $(x_{\text{O}} - \frac{2}{5}) = k(x_{\text{Li}} - \frac{2}{5})$. Using unit weights in the data of Table 2, the fitted value is $k = -0.271(2)$ and the linear correlation coefficient value is $r = 0.9966$.

Since the range of the solid solution is also represented by a straight line $x_{\text{O}} = \frac{1}{2}$ (along $\text{Li}_2\text{O}_2\text{--CuO}$), the point of intersection between these two lines corresponds to the composition of the solid solution $\text{Li}_x\text{Cu}_{1-x}\text{O}$ in the two-phase area together with Li_2CuO_2 . The analytical result is $\text{Li}_{0.06}\text{Cu}_{0.94}\text{O}$. This contradicts experimental results where diffraction lines of Li_2CuO_2 occur even at a nominal starting composition of $\text{Li}:\text{Cu} = 0.03:0.97$.

However, after heating for 1–2 days at 1100 K the Li_2CuO_2 phase disappears and a new phase forms. Therefore, the tie-line as determined by TG/DTA reflects a metastable situation. The value of 6% lithium in CuO thus represents the maximum supersaturation at this temperature.

On increasing the temperature in the TG/DTA experiment, further mass losses occur although now to a much more limited extent and without reaching any well-defined plateau. Diffraction analysis performed by sampling at constant temperature does not give a clear picture of what is occurring in detail at approxi-

mately 1135 K, except that a new phase begins to form. The composition probably lies near LiCu_3O_3 . The endothermic heat effect at this temperature is, with the resolution available, fairly constant within the composition series and cannot be taken as a proper measure of the amount of this phase. In some samples yet another new phase, " LiCu_2O_2 ", is also present as an intermediate product before all the Li_2CuO_2 has disappeared. Although " LiCu_3O_3 " and $\text{Li}_x\text{Cu}_{1-x}\text{O}$ appear to be the stable products at approximately 1175 K, the mass loss at still higher temperatures appears to involve some lithium-containing species, for prolonged heating eventually produces a single-phase specimen of $\text{Li}_x\text{Cu}_{1-x}\text{O}$.

3.3. New ternary phases

Diffraction lines belonging to an unknown product were observed for $\text{Li}_2\text{CO}_3/\text{CuO}$ mixtures which had been heat-treated and quenched from 1100 K (for lithium contents greater than 10%). This pattern dominated when the lithium content was further increased towards 25%. We tentatively call this phase LiCu_3O_3 . However, lack of reproducibility when varying Li/Cu ratios, temperatures and holding times made it difficult to optimize the conditions for obtaining it.

The pattern was successfully indexed on a primitive tetragonal cell, $a \approx 2.8 \text{ \AA}$ and $c \approx 8.9 \text{ \AA}$, the exact values depending on the synthesis conditions (see Table 3). However, complementary X-ray and electron diffraction studies on single-crystal material indicate that the true cell is twice as large—a factor of $\sqrt{2}$ compared with

TABLE 3

X-ray diffraction data as obtained by Cu $K\alpha_1$ radiation for " LiCu_3O_3 " chemically isolated from a mixture with Li_2CuO_2 (see text). The intensities were measured densitometrically from a Guinier film. The refined cell parameters on a tetragonal model are $a = 2.8139(2) \text{ \AA}$ and $c = 8.8777(6) \text{ \AA}$. The result from a preparation in a closed silver tube are $a = 2.8127(2) \text{ \AA}$ and $c = 8.967(2) \text{ \AA}$. The observed and calculated values corresponding with the interplanar spacings are given as $Q = d^{-2} \text{ \AA}^{-2}$. The intensity scale is relative with the maximum set at 100

h	k	l	Q_{obs}	Q_{calc}	I_{obs}	h	k	l	Q_{obs}	Q_{calc}	I_{obs}
0	0	1	0.01267	0.01269	5	2	0	0	0.50514	0.50517	62
0	0	2	0.05076	0.05075	6	2	0	2	0.55588	0.55592	3
0	0	3	0.11413	0.11419	16	1	1	5	0.56978	0.56979	10
1	0	0	0.12629	0.12629	22	1	0	6	0.58297	0.58306	38
1	0	1	0.13892	0.13898	11	2	0	3	0.61944	0.61937	10
1	0	2	0.17706	0.17705	100	0	0	7	0.62155	0.62172	4
0	0	4	0.20287	0.20301	55	2	1	0	0.63156	0.63147	6
1	0	3	0.24036	0.24049	9	2	1	1	overlap Si	0.64431	2
1	1	0	0.25243	0.25259	100	2	1	2	0.68225	0.68222	68
1	1	1	0.26504	0.26527	2	2	0	4	0.70822	0.70818	61
1	1	2	0.30319	0.30334	4	2	1	3	0.74587	0.74566	7
0	0	5	0.31708	0.31720	6	1	0	7	0.74787	0.74801	5
1	0	4	0.32920	0.32930	9	0	0	8	0.81243	0.81204	11
1	1	3	0.36666	0.36678	11	2	0	5	0.82237	0.82237	6
1	1	4	0.45545	0.45560	75						

the short-axes values. Convergent beam patterns support the view that the symmetry is tetragonal. However, extensive disorder observed in the high-resolution electronmicrographs makes it difficult to draw a decisive conclusion.

Similar reproducibility problems occur for the second new ternary phase which forms at higher temperatures and high lithium contents ("LiCu₂O₂"). Here too the conditions for obtaining a single-phase specimen have not been attained; LiCu₂O₂ was found together with Li₂CuO₂, Li_xCu_{1-x}O and LiCu₃O₃. A tetragonal indexing of the powder pattern seemed applicable at first, but on films of better line quality a noticeable line-splitting at $d \approx 1.43 \text{ \AA}$ suggested a lowering of symmetry to an orthorhombic cell, $a = 5.729 \text{ \AA}$, $b = 5.717 \text{ \AA}$ and $c = 12.411 \text{ \AA}$. However, for such a cell many powder lines were missing.

While one selected single-crystal showed tetragonal symmetry, another crystal from the same batch showed orthorhombic symmetry in agreement with the powder diffraction data. Again, electron diffraction hinted that the true cell might even be a modification of the orthorhombic one given above. It is possible to index all powder lines by making one axis one-half of the previous value. As can be seen in Table 4, where the results from two different specimens are given, the axis ratio lies very near 2. This may make intergrowth/twinning easy. Depending on the ratio between members of different orientations, *virtual* tetragonal or orthorhombic symmetry (with $a \approx b$) is obtained for the crystals. Further work with HREM is in progress.

Although neither of the two new ternary phases was obtained in pure form through direct synthesis, they could be isolated in powder form from binary mixtures containing Li₂CuO₂. The latter reacts with water to form Cu(OH)₂. By using aqueous ammonia, the decomposition products remain in solution. The two new ternary phases may thus be filtered off, leaving Li⁺ and copper ammine complexes in solution. Powder compacts of LiCu₃O₃ and LiCu₂O₂ isolated in this manner were used for determining the electrical properties. The temperature dependence of the resistivity for LiCu₃O₃ seems to be that of "hopping conduction" (Fig. 3). Since thin crystal plates which had never been in contact with water gave similar results (which could not be put on an absolute scale owing to inherent large errors in measuring the dimensions), any possibility of incorporated H₂O or OH⁻ must be excluded. The Seebeck effect is positive and increases with temperature (Fig. 4). The resistivity for LiCu₂O₂ is considerably larger and could not be determined properly.

As observed from TG/DTA and indicated by high-temperature X-ray diffraction, both phases decompose (below 650 K) when heated in oxygen. Oxygen is taken up, bringing all the copper to divalency. For the tetragonal phase, a mass increase of 3.22% was observed, in good agreement with the theoretical value of 3.26% expected for oxidation of LiCu₂^ICu^IO₃. These data and results of preliminary structural work, which must be continued on better material, are suggestive of a Cu^I/Cu^{II} ratio of 1:2 and 1:1, respectively, for the two new phases.

3.4. Li₃Cu₂O₄

The compound was obtained in a mixture together with Li₂CuO₂ and Li_xCu_{1-x}O. The diffraction lines could be identified as those given by Klemm *et al.*

TABLE 4

X-ray powder diffraction data of “ LiCu_3O_2 ” interpreted on a primitive orthorhombic cell with $a/b \approx 2$. The refined cell parameters are $a = 5.730(1) \text{ \AA}$, $b = 2.8606(4) \text{ \AA}$, $c = 12.417(2) \text{ \AA}$; $a/b = 2.0033(5)$. The cell was also determined for a sample prepared in a silver container: $a = 5.716(1) \text{ \AA}$, $b = 2.8604(6) \text{ \AA}$, $c = 12.516(2) \text{ \AA}$; $a/b = 1.9982(6)$. Both samples also contained “ LiCu_3O_3 ” and $\text{Li}_x\text{Cu}_{1-x}\text{O}$

<i>h k l</i>	<i>Q</i> _{obs}	<i>Q</i> _{calc}	Int.	<i>h k l</i>	<i>Q</i> _{obs}	<i>Q</i> _{calc}	Int.
0 0 2	0.02592	0.02594	15	2 1 6	0.47739	0.47749	51
1 0 1	0.03693	0.03694	37	4 0 0	0.48737	0.48724	35
1 0 2	0.05641	0.05639	38	0 2 0	0.48920	0.48883	15
0 0 4	0.10375	0.10377	4	3 1 4	0.50081	0.50009	2
0 1 1	0.12858	0.12869	34	4 0 2	0.51362	0.51326	4
2 0 1		0.12831		0 2 2		0.51476	
1 0 4	0.13413	0.13422	4	1 2 1	0.52542	0.52576	5
1 1 1	0.15922	0.15914	15	1 2 2	0.54493	0.54522	5
1 1 2	0.17894	0.17860	37	3 1 5	0.55846	0.55841	4
2 0 3		0.18020		1 1 8	0.56747	0.56776	5
0 1 3	0.18045	0.18058	100	4 1 1	0.61621	0.61601	7
1 0 5	0.19244	0.19259	13	2 2 1		0.61713	
0 0 6	0.23335	0.23347	43	2 0 9		0.64718	
2 1 0	0.24404	0.24402	89	0 1 9	0.64752	0.64752	20
1 1 4	0.25638	0.25643	5	0 0 10		0.64854	
2 1 2	0.26995	0.26998	10	2 1 8	0.65855	0.65908	10
2 0 5	0.28386	0.28394	20	4 1 3	0.66868	0.66781	43
3 0 2	0.29999	0.30001	9	2 2 3		0.66900	
1 1 5	0.31502	0.31479	19	1 2 5	0.68062	0.68142	4
3 0 4	0.37829	0.37789	4	4 0 6	0.72086	0.72071	13
3 1 1	0.40242	0.40281	4	0 2 6	0.72253	0.72230	13
0 0 8	0.41540	0.41506	5	4 1 5	0.77247	0.77167	9
3 1 2	0.42224	0.42222	6	2 2 5		0.77279	
3 0 5	overlap	0.43621		3 2 2	0.78892	0.78888	3
2 0 7	0.43978	0.43964	6	3 1 8	0.81286	0.81141	4
0 1 7		0.44001					

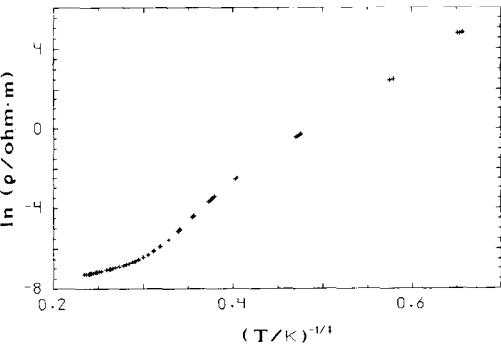


Fig. 3. The temperature dependence of the electrical resistivity for LiCu_3O_3 .

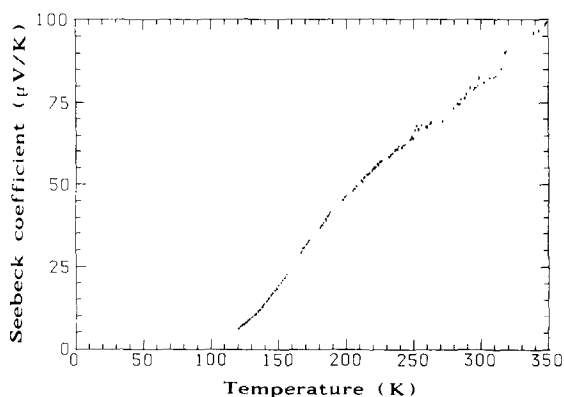


Fig. 4. The temperature dependence of the Seebeck coefficient for LiCu_3O_3 .

[9] in the form of a line diagram. Isolation by ammonia treatment was not possible here since the compound itself reacts with water. The Q -values of lines that most certainly belong to this phase were measured and were fed into an indexing program, TREOR [20]. The most satisfactory solution corresponded to a monoclinic cell. Considering the indices found, and the short b axis, a probable space-group assignment is $C2/m$. A calculation of the theoretical density using two formula units of $\text{Li}_3\text{Cu}_2\text{O}_4$ to the cell gives a value of 4.0 g cm^{-3} , which seems very reasonable in view of the values of other phases in the system. X-ray diffraction data are given in Table 5.

The value of the unique axis is of the same magnitude as found for NaCuO_2 [11], where all copper is trivalent, and is only slightly shorter than in Li_2CuO_2 . In fact, a comparison with the latter is interesting, since a C-centred monoclinic cell can be devised with dimensions rather similar to those of the cell suggested for $\text{Li}_3\text{Cu}_2\text{O}_4$. In order to attain the correct stoichiometry, less lithium is required, three-quarters of the content in Li_2CuO_2 . At present the data are too limited to allow for a solution of the structure from powder diffraction.

4. Conclusions

The Li–Cu–O system revisited has revealed two new ternary phases (tentatively LiCu_3O_3 and LiCu_2O_2), stable only at elevated temperatures, which both seem to contain a mixture of Cu^{I} and Cu^{II} . One example from nature is the very rare mineral paramelaconite with the composition Cu_4O_3 [21]. The mixed valency probably represents a metastable state at ambient temperature and oxygen partial pressure in all these cases, which may explain the scarcity of the mineral and the fact that it is always found together with tenorite (CuO).

Lithium substitution in CuO produces a small concentration of positive charge carriers, as seen from the sign of the Seebeck coefficient. The resistivity is rather high which accentuates the localized character of oxygen holes formed.

TABLE 5

X-ray powder diffraction data of $\text{Li}_3\text{Cu}_2\text{O}_4$ interpreted on a C-centred monoclinic cell with dimensions $a = 9.958(2) \text{ \AA}$, $b = 2.7770(4) \text{ \AA}$, $c = 7.281(1) \text{ \AA}$ and $\beta = 118.77(1)^\circ$, compared with previous data from Klemm *et al.* [9] as measured with a ruler from the diffraction line diagram in their publication. The first 15 Q_{calc} values given are all the reflections expected (up to $\Theta = 21.20^\circ$) from this monoclinic model. The line positions and intensities were measured by a computer controlled microdensitometer from a film including silicon lines. Too weak lines, or those overlapped by $\text{Li}_x\text{Cu}_{1-x}\text{O}$ or Li_2CuO_2 present in the sample, were not measurable

$h k l$	Q_{obs}	Q_{calc}	I_{obs}	d_{obs}	d_{obs} [9]	I_{obs} [9]
0 0 1	0.02465	0.02453	5	6.37	6.4	20
-2 0 1	0.04241	0.04248	100	4.86	4.85	100
2 0 0	0.05249	0.05250	17	4.36	4.35	60
-2 0 2		0.08152				
0 0 2	0.09836	0.09810	52	3.19	3.20	100
2 0 1	0.11140	0.11157	54	3.00	2.98	100
1 1 0	0.14271	0.14278	7	2.647		
-1 1 1	0.15001	0.15003	12	2.582	2.56	30
-4 0 1	0.16559	0.16544	5	2.457		
-2 0 3	0.16967	0.16960	16	2.428	2.43	30
-4 0 2		0.16993				
1 1 1	overlap	0.18459	(CuO)		2.32	40
-1 1 2	0.20634	0.20634	10	2.201	2.21	30
4 0 0	0.21016	0.21000	2	2.181		
2 0 2	0.21959	0.21968	5	2.134	2.13	40
-3 1 1	0.22015	0.22049	9	2.131		
-3 1 2	0.24244	0.24225	58	2.032	2.02	100
-3 1 3	0.31304	0.31306	18	1.788	1.79	60
-4 0 4	0.32625	0.32607	3	1.751	1.75	10
-6 0 2	0.36315	0.36335	2	1.659	1.66	10
2 0 3	0.37694	0.37685	6	1.629		
-6 0 3	0.38244	0.38235	3	1.617	1.62	5
-5 1 1	0.39582	0.39595	36	1.589	1.59	80
-5 1 3	0.41967	0.41944	10	1.544	1.54	30
-3 1 4	0.43300	0.43293	5	1.520	1.52	20
-6 0 4	0.45033	0.45040	8	1.490	1.49	20
-1 1 4	0.46591	0.46609	17	1.465	1.46	30
-2 0 5	overlap	0.49292	(CuO)		1.42	5
0 2 0	0.51857	0.51860	13	1.389	1.39	30
-6 0 5	0.56747	0.56750	7	1.327		
5 1 1	0.56858	0.56865	7	1.326		
4 2 0	0.72891	0.72860	12	1.171		
5 1 2		0.72855				
-4 2 3	0.74186	0.74208	5	1.161		

In this paper a suggestion is also given as to the indexing of $\text{Li}_3\text{Cu}_2\text{O}_4$ where mixed valency again occurs, this time $\text{Cu}^{\text{II}}/\text{Cu}^{\text{III}}$. On the basis of the cell dimensions and the centring of the monoclinic cell, a close structural relationship with Li_2CuO_2 is anticipated.

Work is in progress on further structural characterization of the two new phases as well as of $\text{Li}_3\text{Cu}_2\text{O}_4$.

Acknowledgments

The author gratefully acknowledges the free-of-leave granted by the University of Uppsala, Sweden, to permit a temporary position in Groningen, financed by The Netherlands Foundation for Pure Research (NWO/SON). The experimental work was possible by financial and technical aid from The Solid State Group of the Inorganic Department. Silver tubing was kindly supplied by Professor A. Simon, Max-Planck-Institut für Festkörperforschung, Stuttgart. The TG/DTA investigations were performed at Intechmij, Diemen, through the cooperation by Mr. N. Porsius and Mr. W. Veenstra. Preliminary electron and X-ray diffraction data were obtained by Drs. M. Sundberg and L. Eriksson, Stockholm, and by Drs. A. Meetsma, J. de Boer and P. Bronsveld, Groningen.

References

- 1 K. Hauffe and H. Grunewald, *Z. Phys. Chem.*, **198** (1951) 248.
- 2 R. R. Heikes and W. D. Johnston, *J. Chem. Phys.*, **26** (1957) 582.
- 3 A. V. Silakov, G. S. Tyurikov and N. P. Vasilistov, *Sov. Phys. Inorg. Mater.*, **5** (1970) 2221.
- 4 W. Losert and R. Hoppe, *Z. Anorg. Allg. Chem.*, **515** (1984) 95.
- 5 R. Hoffmann, R. Hoppe and W. Schäfer, *Z. Anorg. Allg. Chem.*, **578** (1989) 18.
- 6 W. Losert and R. Hoppe, *Z. Anorg. Allg. Chem.*, **524** (1985) 7.
- 7 H. N. Migeon, A. Courtois, M. Zanne, C. Gleitzer and J. Aubry, *Rev. Chim. Minér.*, **12** (1975) 203.
- 8 R. Hoppe and H. Rieck, *Z. Anorg. Allg. Chem.*, **379** (1970) 157.
- 9 W. Klemm, G. Wehrmeyer and H. Bade, *Z. Elektrochem., Ber. Bunsenges. Phys. Chem.*, **63** (1959) 56.
- 10 A. R. Wizansky, P. E. Rauch and F. Disalvo, *J. Solid State Chem.*, **81** (1989) 203.
- 11 N. Brese, M. O'Keeffe, R. B. von Dreele and V. G. Young, Jr., *J. Solid State Chem.*, **83** (1989) 1.
- 12 M. Deutsch and M. Hart, *Phys. Rev. B*, **26** (1982) 5558.
- 13 R. Berger and C. F. van Bruggen, *J. Less-Common Met.*, **113** (1985) 291.
- 14 B. X. Yang, T. R. Thurston, J. M. Tranquada and G. Shirane, *Phys. Rev. B*, **39** (1989) 4343.
- 15 B. Roden, E. Braun and A. Freimuth, *Solid State Commun.*, **64** (1987) 1051.
- 16 S. Åsbrink and L. J. Norrby, *Acta Crystallogr. B*, **26** (1970) 8.
- 17 W. De Sisto, B. T. Collins, R. Kershaw, K. Dwight and A. Wold, *Mater. Res. Bull.*, **24** (1989) 1005.
- 18 A. Junod, D. Eckert, G. Triscone, J. Müller and W. Reichardt, *J. Phys.: Condens. Matter*, **1** (1989) 8021.
- 19 *Gmelins Handbuch der anorganischen Chemie*, No. 20, Verlag Chemie, Weinheim, 8th edn., 1960.
- 20 P.-E. Werner, *J. Appl. Crystallogr.*, **18** (1985) 367.
- 21 M. O'Keeffe and J.-O. Bovin, *Amer. Miner.*, **63** (1978) 180.